Editor's Summary

Spot-On Toxicity Testing

"Just a little pinprick," Pink Floyd once reassured its listeners. Of certainty, they were not singing about liver function tests. Nevertheless, the soothing lyric can be just as readily applied to paper-based microfluidics, for which only a droplet of blood––from a finger pinprick––can indicate whether a patient has liver toxicity and needs additional care. In a new study, Pollock and colleagues developed a cost-effective, multiplexed paper-based test that measures two enzymes in human blood commonly associated with liver injury: aspartate aminotransferase (AST) and alanine aminotransferase (ALT).

Levels of these transaminases are elevated in patients with liver toxicity, such as those on several medications at once (for example, drug "cocktails" for HIV and tuberculosis). In the developing world, limited resources often prevent patients from having access to the automated laboratory tests used in developed countries. To address this unmet need, Pollock *et al.* created a point-of-care (POC) device that requires only blood and the human eye for analysis. The authors stacked layers of patterned paper containing "test zones" with chemistries specific for measuring AST and ALT. When blood (<35 μl) is spotted on the device, it interacts with reagents to provide, in 15 min, a colorimetric readout that falls into one of three "bins": <3×, 3×-5×, or >5× the upper limit of normal. This semiquantitative, color-coded message, along with three control zones, informs the doctor of basic facts needed to devise the next treatment steps. Pollock and coauthors tested their paper-based device using 233 blood samples with a range of AST and ALT concentrations. Over all three bins, the device was ≥90% accurate with both serum and whole blood when compared to standard measurement techniques.

Costing only pennies to make, these devices can be used at POC to inform clinicians of possible liver injury, without the long waits for results to return from centralized laboratories. With readouts obtained in near real time, patients all over the world can be comfortably reassured of their health.

A complete electronic version of this article and other services, including high-resolution figures, can be found at:
http://stm.sciencemag.org/content/4/152/152ra129.full.html

Supplementary Material can be found in the online version of this article at:
http://stm.sciencemag.org/content/suppl/2012/09/17/4.152.152ra129.DC1.html

Information about obtaining **reprints** of this article or about obtaining **permission to reproduce this article** in whole or in part can be found at:
http://www.sciencemag.org/about/permissions.dtl

BIOMEDICAL ENGINEERING

A Paper-Based Multiplexed Transaminase Test for Low-Cost, Point-of-Care Liver Function Testing

Nira R. Pollock,[1][*][†] Jason P. Rolland,[2][*][†] Shailendra Kumar,[2] Patrick D. Beattie,[2] Sidhartha Jain,[2] Farzad Noubary,[3] Vicki L. Wong,[2] Rebecca A. Pohlmann,[4] Una S. Ryan,[2] George M. Whitesides[5]

In developed nations, monitoring for drug-induced liver injury through serial measurements of serum transaminases [aspartate aminotransferase (AST) and alanine aminotransferase (ALT)] in at-risk individuals is the standard of care. Despite the need, monitoring for drug-related hepatotoxicity in resource-limited settings is often limited by expense and logistics, even for patients at highest risk. This article describes the development and clinical testing of a paper-based, multiplexed microfluidic assay designed for rapid, semiquantitative measurement of AST and ALT in a fingerstick specimen. Using 223 clinical specimens obtained by venipuncture and 10 fingerstick specimens from healthy volunteers, we have shown that our assay can, in 15 min, provide visual measurements of AST and ALT in whole blood or serum, which allow the user to place those values into one of three readout "bins" [<3× upper limit of normal (ULN), 3 to 5× ULN, and >5× ULN, corresponding to tuberculosis/HIV treatment guidelines] with >90% accuracy. These data suggest that the ultimate point-of-care fingerstick device will have high impact on patient care in low-resource settings.

INTRODUCTION

Blood tests for monitoring the status of the liver are a standard part of medical care in developed nations, particularly for individuals who either have underlying liver disease or are taking medications that can cause hepatotoxicity. Accordingly, U.S. guidelines call for baseline and serial monitoring of serum transaminases, aspartate aminotransferase (AST) and alanine aminotransferase (ALT), in at-risk individuals while on standard therapies for tuberculosis (TB) (1) and/or HIV (2). The overall incidence of clinically relevant hepatotoxicity on TB therapy (typically owing to the medications isoniazid, rifampin, and pyrazinamide) ranges from 2 to 33%, and risk may be increased by multiple factors, such as preexisting liver disease (for example, hepatitis B and/or C), alcohol use, and increasing age (1, 3). Hepatotoxicity associated with nevirapine-based HIV therapy, widely used in the developing world, is of particular concern; rates of nevirapine-associated hepatotoxicity can exceed 13%, depending on underlying risk factors and treatment (2, 4, 5). Simultaneous treatment for both TB and HIV further complicates matters and sometimes generates additive risk of hepatotoxicity (6, 7). In practice, however, it is difficult to predict accurately which patients on treatment will actually develop hepatotoxicity. For example, severe idiosyncratic drug-induced liver injury has been observed in patients with no obvious predictors for isoniazid-associated liver injury who were treated with isoniazid alone for latent TB (8).

Monitoring for hepatotoxicity in resource-limited settings is often limited by relative expense and logistical and practical concerns, even for patients at highest risk. Testing is often done in centralized or re-gional laboratories in these settings, which can delay obtaining and acting on results. Many patients have strong negative feelings about venipuncture itself, and this aversion can be a barrier to care (9). Because of these obstacles, in many resource-limited settings patients with TB and/or HIV receive minimal or no monitoring during treatment. To provide access to affordable point-of-care (POC) screening, without sacrificing the ability to perform clinically useful (and even complex) tests, we (10–15), and others (16–23), have developed microfluidic platforms based on paper (broadly defined as thin porous media). Paper-based microfluidic devices consist of hydrophilic paper channels defined by patterning of hydrophobic barriers (10, 12, 13) or by cutting (16–20, 23). Using these defined channels, we can direct fluid flow toward specific detection zones and perform operations, such as mixing, splitting, and filtration, autonomously.

Unlike traditional POC paper-based devices (for example, lateral flow tests), which typically run one or two tests in series (requiring that each assay on the device be compatible with the others in terms of buffers and other reagents and that assays not cross-react), paper-based microfluidic devices, with their ability to modify and direct flow within microfluidic channels [and in three dimensions (3D)], have the capacity to split a single, low-volume (<40 μl) sample into multiple separate portions, which can each be assayed in parallel. This allows for high-level multiplexing of independently optimized assays with discrete assay conditions and eliminates concern about cross-reactivity between assays. Like lateral flow tests, paper-based microfluidic devices require no external pumps, instrumentation, or power and are both portable and disposable. Paper-based microfluidic technology has been reported for potential clinical diagnostic applications (11–24). These proof-of-principle studies have demonstrated both the ability to conduct clinical chemistry, enzymatic, immunoassay, and enzyme-linked immunosorbent assay tests on patterned paper, visually and quantitatively (the latter through the use of camera-enabled cellphones), and the viability of both single layer (12, 14, 16–24) and 3D (13) patterned paper devices to sense various analytes, including AST (24). However, despite this substantial body of proof-of-concept work, there has been minimal validation of paper-based microfluidic devices using actual

[1]Division of Infectious Diseases, Beth Israel Deaconess Medical Center, 330 Brookline Avenue, Boston, MA 02215, USA. [2]Diagnostics For All, 840 Memorial Drive, Cambridge, MA 02139, USA. [3]Department of General Medicine, Division of Infectious Diseases, Massachusetts General Hospital, 50 Staniford Street, 9th Floor, Boston, MA 02114, USA. [4]Department of Pathology, Beth Israel Deaconess Medical Center, Boston, MA 02215, USA. [5]Department of Chemistry and Chemical Biology, Harvard University, 12 Oxford Street, Cambridge, MA 02138, USA.
*These authors contributed equally to this work.
†To whom correspondence should be addressed. E-mail: jrolland@dfa.org (J.P.R.); npollock@bidmc.harvard.edu (N.R.P.)

clinical specimens, and a field-ready clinical test for monitoring hepatotoxicity has yet to be demonstrated.

Here, we demonstrate major progress toward the development of a paper-based, POC assay for rapid, semiquantitative measurement of AST and ALT in a fingerstick whole-blood specimen. For highest clinical utility, the device has been optimized for visual color readout in AST and ALT ranges, or "bins" [<3× upper limit of normal (ULN), 3 to 5× ULN, and >5× ULN], that correspond to the cutoffs currently used for clinical management decisions per TB (1) and HIV treatment guidelines in the United States (2). Our data suggest that, ultimately, this paper-based fingerstick device could significantly affect patient care, particularly in resource-limited settings.

RESULTS

Design and chemistry of the paper-based transaminase test
The paper-based transaminase test is an example of a 3D device made from layering patterned paper (Fig. 1A). To create a layer of patterned paper, we used a wax-based printer and a heat source to print microfluidic, hydrophilic paths within the paper, through which flow (drawn by wicking) can be directed to specific "detection zones." Layers of patterned paper were stacked to generate 3D devices by depositing patterned layers of hydrophobic adhesive by means of screen printing and adhering multiple sheets together. Our postage stamp–sized device ($20 \times 20 \times 0.5$ mm^3) was designed to perform two separate tests: One zone measures AST and another measures ALT (Fig. 1, B and C) in a clinical sample in 15 min. Additionally, the test contains three control zones to ensure proper device performance (Fig. 1D and fig. S1). Each test zone has a unique environment (pH, buffer, reagents, etc.) that ensures specificity. The AST assay chemistry is based on the sulfonation of methyl green, which results in a visual transformation from blue to pink as the dye becomes colorless and the pink background color (rhodamine B) is revealed (Fig. 1C) (Supplementary Methods). The ALT assay chemistry is based on the conversion of L-alanine to pyruvate, the subsequent oxidation of pyruvate by pyruvate oxidase, and the use by horseradish peroxidase of the liberated hydrogen peroxide to generate a red dye through the coupling of 4-aminoantipyrine and N,N-dimethylaminobenzoic acid (Fig. 1C) (Supplementary Methods).

Our device consists of two layers of similarly patterned paper, a plasma separation membrane, and a laminated cover of polyester film to protect the device from the environment and limit evaporation (Fig. 1A). A hole in the lamination allows for a fingerstick or pipetted drop (30 μl) of whole blood or serum to be applied to the plasma separation membrane (Fig. 1B). If whole blood is applied, blood cells are captured and retained by the plasma separation membrane, whereas plasma wicks into the individual "zones" in the first layer of paper below. In those zones, the plasma fluid reconstitutes dried reagents (required for the zone-specific chemistry) and continues to wick to the second layer of paper, where analytes in the plasma react with additional dried reagents in each detection zone (fig. S1) and generate visual colorimetric signals that can be interpreted and semiquantified with a visual "read guide" (Fig. 1C). The read guide was generated using device images obtained from a desktop scanner and image analysis software (Materials and Methods).

The paper-based transaminase test has several features that inform the user (Fig. 1, C and D). The test has been carefully engineered for visual readout, in that the AST/ALT test zones provide a strong color change across the target clinical range (Fig. 1, C and D). We specifically optimized the interpretable ranges for AST and ALT values (color readouts in the test zones) to correspond to the cutoffs currently used for clinical management decisions per TB treatment guidelines in the United States (1). Accordingly, the results of the test are interpreted as being within one of the following three bins: <3× ULN (0 to 119 U/liter), 3 to 5× ULN (120 to 200 U/liter), or >5× ULN (>200 U/liter) (Fig. 1C). The additional color gradation within each bin on the read guide allows the reader to approximate where within the bin the result lies and thus allows semiquantitative readout. Additionally, three control zones notify the user of insufficient sample volume, hemolysis, or damaged reagents (Fig. 1D); each zone is interpreted as "valid" or "invalid." A result of invalid in any of the three control zones invalidates the entire device.

Analytical performance of the device
Test linearity was measured by adding known amounts of purified ALT and AST to fresh whole human blood, pipetting 30 μl of blood onto the device, and digitizing the color reactions observed after 15 min with a desktop scanner. Image analysis software was used to translate the resulting color intensities in each scanned zone into quantitative information (Supplementary Methods). Both assays were linear across the target clinical range (40 to 200 U/liter), and the 95% prediction intervals showed that, given a particular ALT or AST value, the range of possible color intensities was relatively narrow (Fig. 2, A and B). We determined the limit of detection (LOD) for ALT to be 53 U/liter and for AST to be 84 U/liter in artificial blood plasma buffer (Fig. 2, C and D) (Supplementary Methods). LOD data were fit to the Hill equation, $I = I_{max} [L]^n/([L]^n + [L_{50}]^n)$, by nonlinear regression, where I_{max} is the maximum color intensity, L is AST or ALT concentration (in U/liter), L_{50} is the AST or ALT concentration (in U/liter) that generates a signal equal to one-half of I_{max}, and n is the Hill coefficient (14). For AST, $I_{max} = 105.7$, $L_{50} = 260.9$ U/liter, and $n = 1.72$. For ALT, $I_{max} = 126.5$, $L_{50} = 331.33$ U/liter, and $n = 1.04$. For both assays, the linear portion of the sigmoidal curve ranged from 40 to 200 U/liter.

To measure repeatability of the paper-based test, we measured color intensity for simulated clinical samples: commercial serum samples with known AST/ALT values and fresh whole-blood samples spiked with low/normal ("low") and elevated ("high") levels of AST and ALT (Table 1) (Supplementary Methods). Ten devices were used to measure each sample. Precision was quantified with the coefficient of variation (CV), which is defined as the SD divided by the mean, for each sample. CV values were <10% for both AST and ALT tests in all four conditions (elevated/normal serum/blood) (Table 1).

Device performance with venipuncture clinical specimens
To evaluate the performance of the paper-based transaminase test in actual clinical specimens, we tested aliquots of paired whole-blood and serum specimens that had been drawn simultaneously from patients within the previous 5 hours for routine clinical testing and for which results of automated transaminase testing of the serum specimen were available. Aliquots (30 μl) of blood or serum were applied to each device, and 15 min later, each device was analyzed by three independent, blinded readers. The readers independently matched test zone colors to the closest color/value found on the read guide (Fig. 1C) and recorded a result in units per liter (rounded to the nearest 10 U/liter). Results of the paper-based transaminase test for paired whole-blood and serum specimens were then compared to the results of automated serum transaminase testing as the gold standard (Fig. 3). Unaveraged raw

data are presented in tables S1 to S4. Given that EDTA plasma (separated from cells within 8 hours of collection) is an acceptable alternative specimen for testing by the automated assay, it was assumed that gold standard results for the whole-blood specimen (that is, plasma) would have been equivalent to gold standard results for the paired serum specimen. Whole-blood specimens were discarded after initial testing, whereas serum specimens were stored at 4°C for repeat testing; there was no systematic change in AST or ALT results in either direction (that is, higher or lower) noted on repeat testing of stored serum specimens (tables S3 and S4).
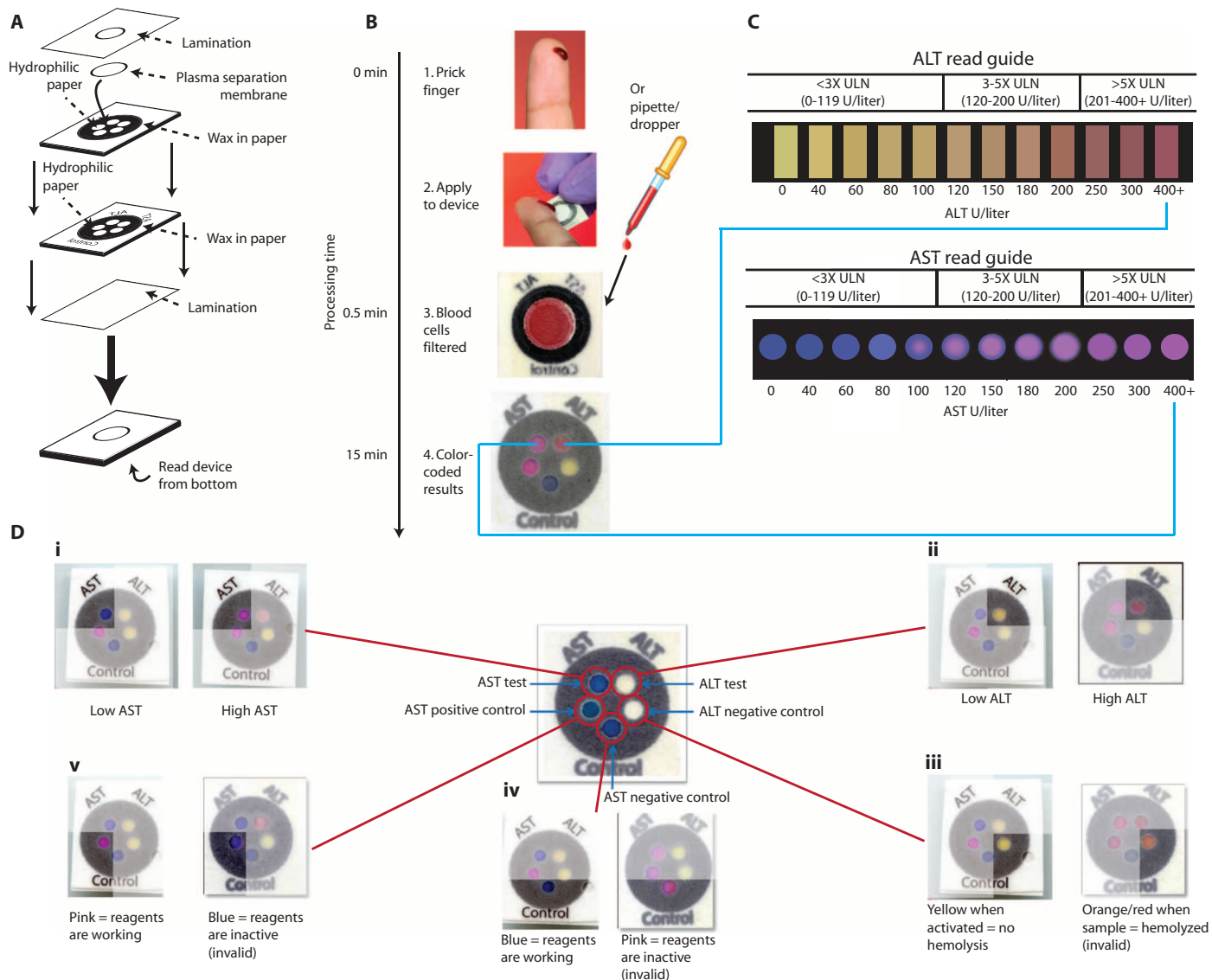
Fig. 1. Schematic of the paper-based AST/ALT test design and protocol. (**A**) The device consists of two layers of similarly patterned paper, a plasma separation membrane, and a laminated cover of polyester film. (**B** and **C**) A drop of whole blood (either a fingerstick specimen or 30 μl of a specimen obtained by venipuncture) is applied to the back of the device. Red and white blood cells are filtered out by the plasma separation membrane, whereas plasma wicks to the five detection zones through patterned hydrophobic channels in the paper (B). After 15 min, the AST and ALT test zones are matched to a color read guide (C) to obtain a concentration value. Results are interpreted as being within one of three bins of values: <3× ULN (ULN defined as 40 U/liter), 3 to 5× ULN, or >5× ULN. (**D**) Detailed schema of the paper-based transaminase test and possible colorimetric readouts for the five zones (i to v). A schematic of test and control zones (before receiving a sample) is shown in the center of the figure. (i) AST test zone: low/normal AST values (<80 U/liter) result in a dark blue color, whereas high AST values (>200 U/liter) result in a bright pink color. (ii) ALT test zone: low/normal ALT values (<60 U/liter) result in a yellow color, whereas high ALT values (>200 U/liter) result in a deep red color. (iii) ALT negative control zone: a change from white to yellow indicates appropriate device activation; in the event of sample hemolysis, the zone becomes orange/red and the device is read as invalid. (iv) AST negative control zone: the baseline blue color remains unchanged if dye chemistry is functioning properly, whereas the zone becomes bright pink in the event of nonspecific dye reaction and the device is read as invalid. (v) AST positive control zone: the zone changes from blue to pink if AST reagents are functioning properly but remains dark blue if either the reagents are not functioning or the zone is not activated, in which case the device is read as invalid.

Bin placement accuracy. Results of the paper-based assay for each specimen were compared to the gold standard automated serum transaminase results to evaluate "bin placement accuracy": whether the result of the paper-based assay was in the same bin (<3× ULN,

3 to 5× ULN, or >5× ULN) as the gold standard result. We calculated bin placement accuracy by determining if each datum met at least one of the following criteria: (i) the value measured by the paper transaminase test was within the correct bin as determined by the automated (true) value or (ii) the value measured by the paper test was within 40 U/liter of the true value. The second criterion accounted for values near the boundaries of the bins, because it was agreed that variations of this magnitude were potentially acceptable because the maximum visual resolution of the device was likely 20 to 30 U/liter and variations of <40 U/liter near these boundaries were unlikely to reflect appreciable differences in clinical status, despite potentially changing management if strict cutoffs at 3× and 5× ULN were to be used for decision-making.

Overall accuracies for the device (data for all three bins in aggregate) were ≥90% for both AST and ALT in both serum and whole blood (Fig. 3 and Table 2). "Per bin" accuracies were calculated by dividing the number of correctly binned samples in each bin by the total number of samples in that bin. ALT accuracies were higher for serum than for whole blood, particularly in the 3 to 5× bin (92% versus 57%, respectively; $P < 0.00003$, χ^2 test). This disparity could be explained by the age of the whole blood (drawn from patient 2 to 5 hours before) at the time of testing. In previous experiments, we found that whole-blood samples with baseline ALT levels less than 40 U/liter began to yield artificially high ALT values (between 120 and 200 U/liter) on the paper test after aging for >6 hours from the time of draw. We believe that this drift in values with age is due to the fact that, over time, red blood cells (RBCs) release lactate, which is then converted to pyruvate; the excess pyruvate leads to activation of the ALT assay and therefore falsely high readings. In the case of serum, RBCs are separated from the serum shortly after draw, preventing accumulation of pyruvate in
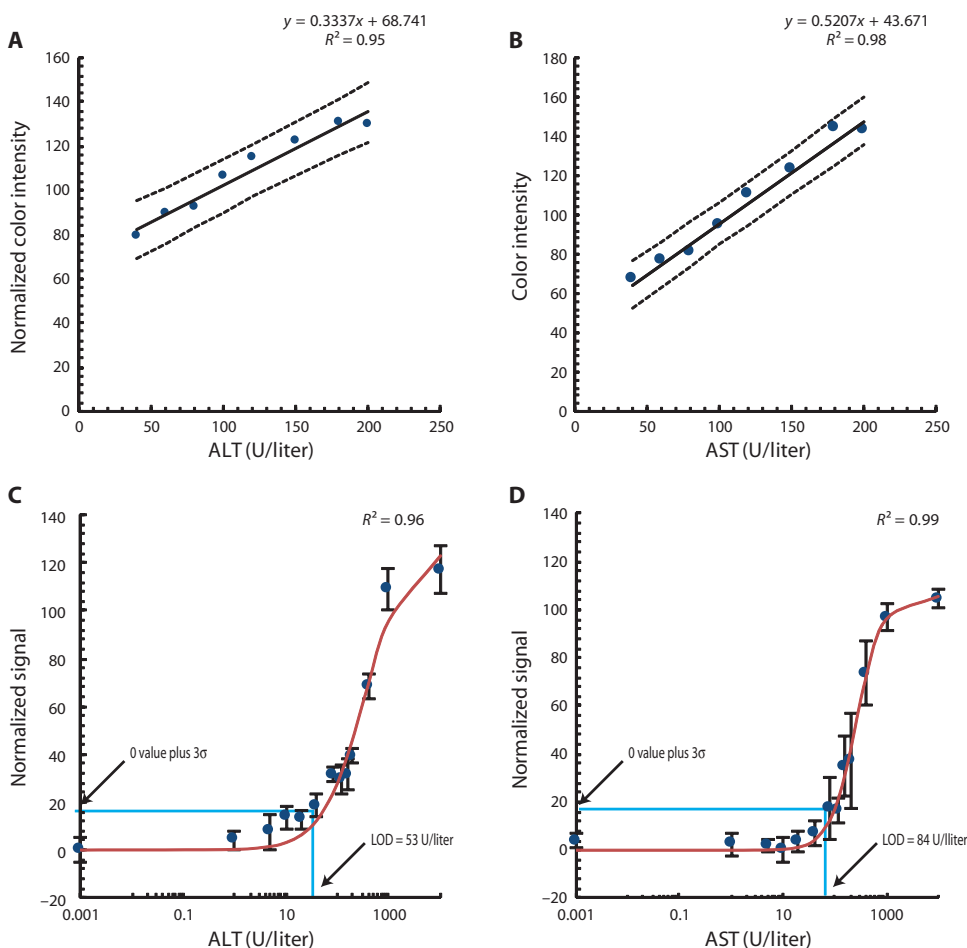

Fig. 2. Paper device performance with ALT and AST spiked into fresh whole human blood. Thirty microliters was pipetted onto each device. (**A** and **B**) Device readout linearity for color intensity versus concentration of ALT (A) or AST (B). Each datum is an average of three independent measurements from three separate devices. Dashed lines represent the upper and lower 95% prediction intervals. ALT values are normalized by subtracting each point from 255 so that higher color intensity values correspond to higher ALT concentrations (Supplementary Methods). (**C** and **D**) LOD curves for ALT (C) and AST (D). Data are normalized such that the lowest intensity measured yields a value of 0 color intensity on the y axis. Solid lines represent a nonlinear regression of the Hill equation. The data are averages of seven measurements ± SD.

Table 1. Repeatability of the paper-based transaminase test. Color intensity was measured and quantified in individual zones. %CV was calculated by dividing the SD by the mean intensity (n = 10 devices per specimen with a given value).

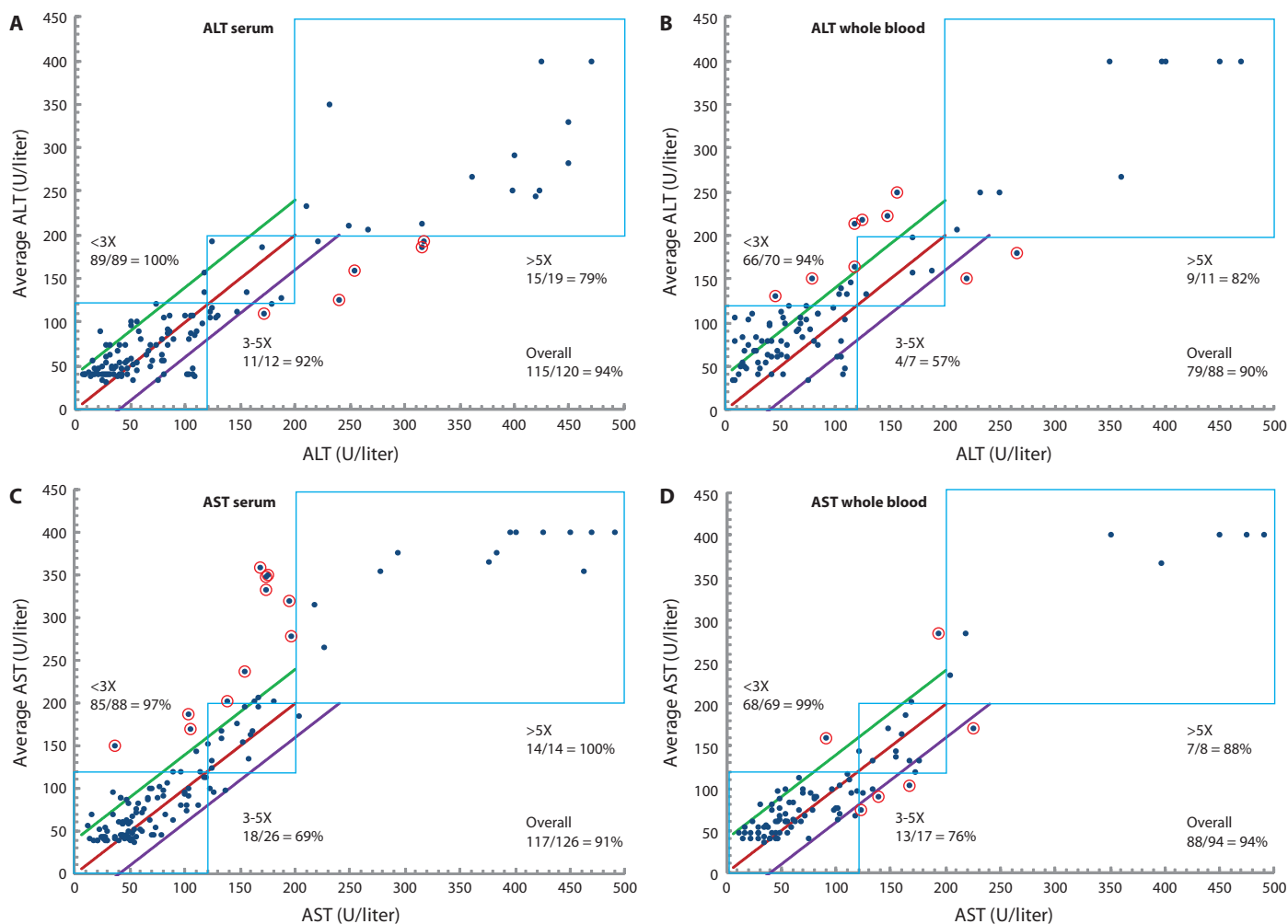|	Serum standard	Serum standard	Whole blood	Whole blood
Actual ALT (U/liter)	56	128	40	200
Actual AST (U/liter)	69	244	40	200
ALT color intensity, mean ± SD (%CV)	111.0 ± 6.55 (5.89)	120.6 ± 11.2 (9.28)	93.6 ± 4.75 (5.08)	146.5 ± 10.59 (7.22)
AST color intensity, mean ± SD (%CV)	62.6 ± 5.52 (8.82)	151.1 ± 7.60 (5.03)	65.3 ± 5.24 (8.01)	168.5 ± 4.45 (2.64)

Fig. 3. Direct comparison of transaminase measurements made with the paper-based device to those made with the standard automated method. (**A** to **D**) ALT values in paired serum (A) and whole-blood (B) clinical specimens and AST values in paired serum (C) and whole-blood (D) clinical specimens are plotted against values (in U/liter) measured in the serum specimen with a gold standard automated method (Roche Modular Analytics System). Results for each whole-blood specimen (*n* = 1 per reader) were averaged from three blinded readers to generate each datum. All serum specimens with sufficient volume remaining after initial testing were stored at 4°C for up to 2.5 weeks and blindly retested in triplicate (three readers blinded to automated results read each serum

of up to three assays performed per specimen) and then averaged. In each plot, the blue boxes represent AST or ALT bins within which values for both the paper-based device and the automated method are within the same range: <3× ULN (0 to 119 U/liter), 3 to 5× ULN (120 to 200 U/liter), or >5× ULN (>200 U/liter). The red line corresponds to the line of equality, and the green and purple lines correspond to ±40 U/liter from the line of equality, respectively. Points circled in red are samples that were neither in the correct bin nor within 40 U/liter of the value measured by the gold standard automated method. For scaling purposes, *x* axis values measured by the Roche system that exceeded 400 U/liter were plotted between 400 and 500 U/liter.

serum. Therefore, we would expect accuracies from fresh whole blood (including from a fingerstick) to mirror the serum results in this study. This hypothesis was preliminarily tested with freshly drawn whole-blood samples with known amounts of ALT added (Fig. 2A), which did not generate falsely high results. (Notably, this effect is not seen in commercial assays because these assays measure the kinetic rate of color formation after the native pyruvate is consumed during an initial incubation period.)

Results for the paper-based test that were neither within the correct bin nor within 40 U/liter of the gold standard result were considered inaccurate (Fig. 3). It is important to note that although all samples

with ALT/AST values below the calculated LODs (53 and 84 U/liter for ALT and AST, respectively) could potentially yield equivalent results from the colorimetric test, some color resolution is lost when scanning the devices and this results in conservatively calculated LOD values. Therefore, attempts to visually distinguish values below the calculated LODs were allowed [discernible color changes made it possible, in principle, to discriminate lower values (Fig. 1C)]. Regardless, these values are well within the <3× ULN range and no clinical action would be expected for the target patient population. Because the device is meant to detect substantially elevated (>3× ULN) transaminase levels, the assay chemistry was tailored to exhibit the greatest color

Table 2. Bin placement accuracies for visual measurements in clinical specimens made with the paper-based transaminase test. Ninety-five percent confidence intervals around the overall accuracy estimates are shown. For the bins, X = 40 U/liter = ULN.

Test	Specimen	Bin	*n* samples in bin	*n* correctly placed	Per bin accuracy (%)	Overall accuracy (%)
ALT	Serum	<3×	89	88	99	95 ± 4
		3–5×	12	11	92	
		>5×	19	15	79	
	Blood	<3×	70	66	94	90 ± 6
		3–5×	7	4	57	
		>5×	11	9	82	
AST	Serum	<3×	88	85	97	91 ± 5
		3–5×	26	18	69	
		>5×	14	14	100	
	Blood	<3×	69	68	99	94 ± 5
		3–5×	17	13	76	
		>5×	8	7	88	

changes between 3× and 5× ULN. Values well above 5× ULN, being out of the linear range, will appear the same on the test and will thus prompt the same clinical response. Notably, the measuring range for the automated assay we used was 4 to 400 U/liter (0.1 to 10× ULN); higher values must be measured by sample dilution.

Method comparison (Bland-Altman analysis). We further evaluated the paper-based device performance by Bland-Altman analysis (*25*) (Supplementary Methods). Specifically, we compared the semicontinuous data (reader estimates, to the nearest 10 U/liter) to the continuous data obtained by gold standard automated testing (Fig. 4). The goal of this analysis was to obtain a more highly resolved assessment of agreement with the gold standard method and to explore device bias and variability in the target clinical range (defined for this analysis as 40 to 250 U/liter). For serum ALT and AST values, we applied a log transformation to our data because the Bland-Altman plot of the untransformed data showed an increase in variability of the differences with increasing magnitude of measurement (Fig. 4, A and B). The log-transformed Bland-Altman plots for ALT and AST serum successfully removed the relationship between differences and the mean (Fig. 4, C and D).

The data were then back-transformed to give values relating to the ratio of the untransformed measurements. The paper-based test underestimated ALT serum by 9% on average, and the 95% limits of agreement were between 60% lower and 90% higher for ALT serum. After the same transformation, AST serum results revealed that the paper-based test overestimated AST serum by 12% on average and the 95% limits of agreement were between 63% lower and 100% higher. We observed a bias of the paper-based device to overestimate the ALT whole-blood data by 18 U/liter, on average (Fig. 4E) (likely due to pyruvate generation). The 95% limits of agreement (the interval expected to contain 95% of paired differences) range from −63 to +99 U/liter for the ALT whole-blood data set. The AST whole-blood plot shows virtually zero bias and 95% limits of agreement from −59 to +62 U/liter (Fig. 4F). Because the differences between color swatches on the read guide are each 20 to 30 U/liter, we expect that the maximum resolution of the device is similarly 20 to 30 U/liter. These results suggest clinically acceptable

agreement between the semiquantitative paper test and the gold standard automated assay method.

Performance of the device in fingerstick testing
We have conducted initial experiments to observe the performance of the device with whole blood obtained through fingerstick. In a small study, a droplet (~30 μl) of blood from a fingerstick was obtained from 10 healthy volunteers and introduced to the paper device. All 10 devices were found to fully activate, meaning that all zones were wet with plasma, and all controls worked properly. As expected for healthy subjects, AST and ALT levels were found to be ≤40 U/liter for all volunteers and matched results of automated testing (Table 3). It is important to note that others have shown equivalency between transaminase levels measured (by automated methods) in whole blood obtained through fingerstick and levels measured in whole blood obtained through venipuncture (*26*, *27*). We therefore similarly expect that, for the paper-based test, fingerstick data for patients with abnormal transaminase levels will demonstrate accuracy comparable to the data presented here for samples collected by venipuncture.

Evaluation of analytes with potential for assay interference
Studies were performed to assess common substances that are present in whole blood and could potentially interfere with ALT and AST assays (fig. S2). Our data suggest that pyruvic acid and ascorbic acid interfere with the ALT assay but not the AST assay. Specifically, pyruvate present at levels >0.2 mM may produce falsely elevated results in the ALT assay, and ascorbic acid present at levels >3 mg/dl may produce falsely low ALT results. All of the other substances tested showed no significant interference (defined as a 10% or greater change in color intensity from the value measured in the specimen containing zero added interferent) in the ALT and AST assays at physiologically relevant levels, including bilirubin (<10 mg/dl), cholesterol (<500 mg/dl), glucose (<1000 mg/dl), lactate (<200 mg/dl), urea (<100 mg/dl), creatinine (<15 mg/dl), and hemoglobin (<120 mg/dl) (fig. S2). These results are consistent with our observations that the paper-based transaminase test performed well in the specimens from the clinically diverse population
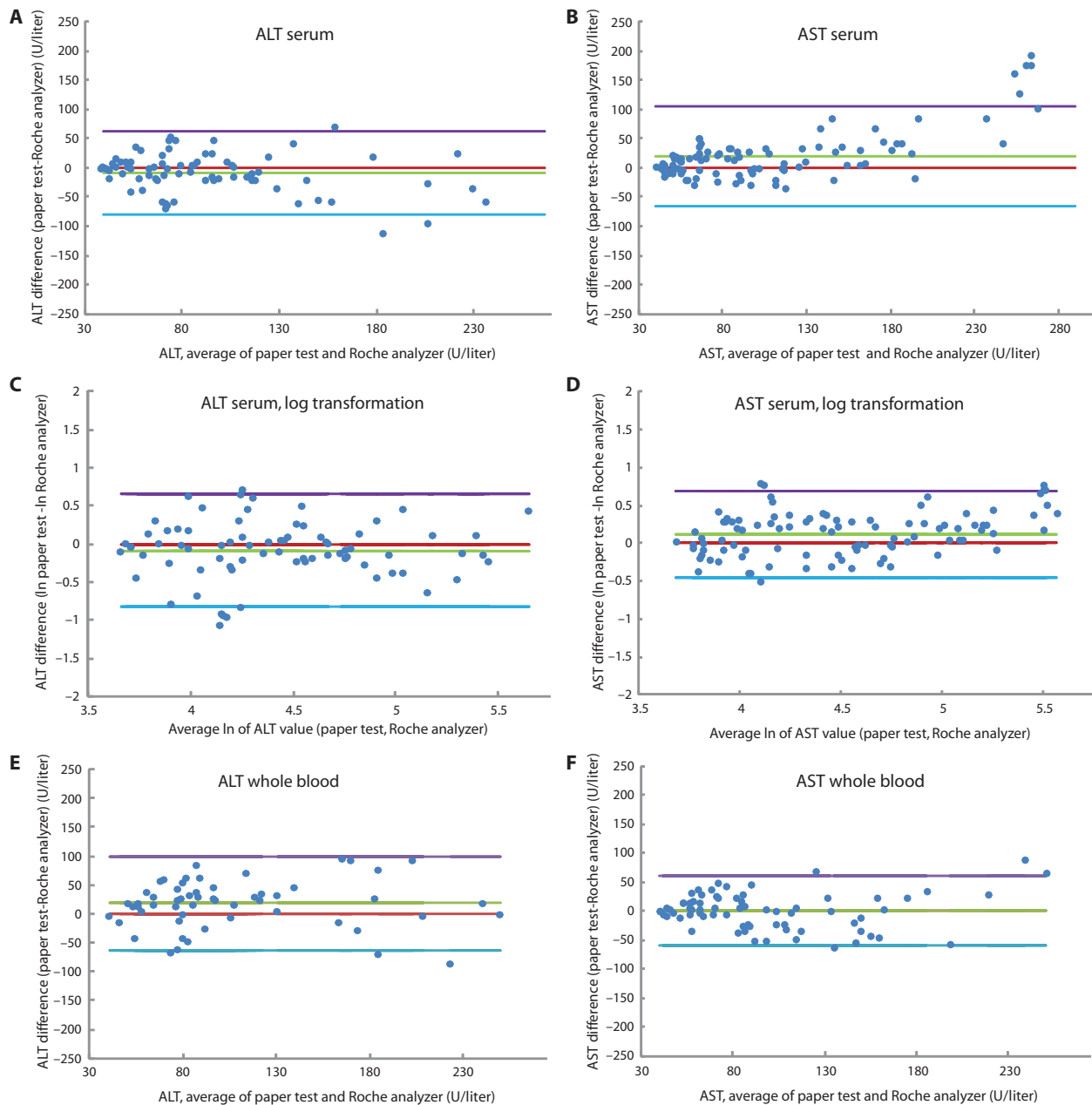
Fig. 4. Bland-Altman plots of visual transaminase measurements in clinical specimens. (**A**) ALT values in serum. (**B**) AST values in serum. (**C**) ALT values in serum (after log transformation). (**D**) AST values in serum (after log transformation). (**E**) ALT values in whole blood. (**F**) AST values in whole blood. The purple and blue lines represent the 95% limits of agreement. The red line is the line of equality, and the green line is the average difference of the methods. Values are derived from the difference between the gold standard method (Roche) and the paper test value (average of all recorded values per sample) (Supplementary Methods).

tested in this study, which included many patients who were critically ill with multiorgan failure and consequently multiple abnormal laboratory values (particularly bilirubin and creatinine).

Assay temperature and read time

Fluctuations in temperature affect the speed of the test, most likely owing to faster enzymatic reactions at higher temperatures (>30°C). Our data indicate reliable performance of the paper-based transaminase test as performed at room temperature (22 to 30°C) and read at 15 min. In the case of higher temperatures (31 to 37°C), the test should be read at 12 min to obtain comparable results (fig. S3).

Effects of blood volume on assay performance

Different volumes (15, 20, 25, 30, 35, 40, and 50 μl) of blood, serum, or buffer specimens with different AST and ALT concentrations were evaluated. We found that at least 25 μl of sample is required for consistent

Table 3. Results from fingerstick testing in 10 healthy volunteers comparing the paper-based test with an automated POC system (Cholestech LDX).

Volunteer	Paper test (U/liter)		Cholestech LDX (U/liter)	
	ALT	AST	ALT	AST
1	40	40	22	29
2	40	40	22	25
3	40	40	23	26
4	40	40	41	35
5	20	40	27	36
6	20	40	18	23
7	20	40	18	17
8	40	40	45	35
9	20	40	17	18
10	20	40	29	25

and complete activation of the devices. Bland-Altman plots were generated to compare data from 35 µl of sample volume with data from 50 µl of sample volume within the clinical range of interest (fig. S4). The data show negligible bias for both ALT and AST assays and acceptable limits of agreement between the two assay volumes. We therefore concluded that excess fluid does not alter the performance of the test, presumably because the paper device can only absorb a finite amount of fluid sample. Insufficient sample results in failure of the negative control spot to turn from white to yellow (Fig. 1D). Applying the appropriate amount of sample can be easily monitored in a field setting by adding blood until the filter is fully saturated (red color is observed across the entire filter) or by using a capillary tube to apply a defined volume.

Assay stability

Stability of the paper-based transaminase test was evaluated by fabricating a single lot of devices and packaging them in heat-sealed, foil-lined pouches (10 tests per pouch) containing a silica desiccant packet. Pouches were stored at 25°C and periodically opened to evaluate the devices with buffer standards. Color intensity of the assays did not vary by more than 8% after a period of 11 weeks, at which point the study was concluded (fig. S5). This value is less than the %CV measured for the assays (Table 1), so the deviation may be attributed to device variability rather than reagent degradation.

DISCUSSION

We have demonstrated that we can accurately measure transaminases in whole blood and serum using a simple and inexpensive paper-based assay that can be read by eye within minutes. Our test performed well compared to automated methods, even in specimens that were obtained from critically ill patients with multiple derangements in other analytes and that were up to 5 hours old at the time of testing. Variability, as measured by %CV, was found to be less than 10% for both assays with blood and serum samples. The experiments presented here have firmly established proof of concept and clinical relevance and

will allow us to move into clinical field studies to evaluate the performance of our device in real time using fingerstick blood specimens from those patients for whom we see the device having highest utility, including those with TB, HIV, hepatitis B, and hepatitis C.

When sufficient resources are available, standard-of-care transaminase testing typically involves collecting a whole-blood specimen by venipuncture, transporting the specimen to a central laboratory, centrifuging to separate serum, and testing the serum on a large automated platform. Such systems are impractically expensive for routine use in developing countries and require highly trained technicians for testing and maintenance. Moreover, the need to perform the testing in a central laboratory can considerably delay acquisition and dissemination of results, even if access to testing is available. In some resource-limited settings, it is not uncommon for tubes to get lost en route to the central laboratory, and transaminase results can sometimes take weeks or even months to return.

Two U.S. Food and Drug Administration–approved devices exist from Roche and Cholestech that could potentially be used for rapid POC testing, but both are arguably too expensive for use in a resource-limited setting. The Roche Reflotron Plus device requires venous blood draw, relies on complex electronics and electricity/battery, and costs about $6000 for the reader and an additional $4 per test. The other device, the Cholestech LDX, is capable of using fingerstick samples but costs about $3000 for the reader and $4 per test. Manufacturing costs for our device are dependent on several key variables, including location, making them difficult to calculate accurately a priori. We anticipate, however, that our device can ultimately be produced at a very low cost—on the order of <$0.10 per test (table S5).

Our platform offers several technical advantages over other platforms developed with paper-based microfluidic technology. The 3D, multi-layered design of our platform allows it to split a single 30- to 35-µl sample of whole blood into five separate "streams" of plasma, which are tested with five independently optimized assays in parallel, in 15 min, at ambient temperature. There is no requirement for preanalytical sample processing or for the addition of any other reagents once the sample is added to the device, and no requirement for equipment to read the device, and thus operation of the device will require only tools to obtain and apply the blood sample (that is, a lancet and potentially a capillary tube).

Our test has been optimized for detection of AST and ALT values >3× ULN, in light of guidelines (1, 2) that place great emphasis on the 3× ULN (in concert with symptoms of hepatotoxicity) and 5× ULN cutoffs for making management decisions. Although we hope to have sufficient resolution in the 3 to 5× range to allow highly accurate bin placement, we also believe that our test could have great benefit as a "rule-out" or "triage" test. For instance, if values on the POC test were ≥3× ULN, the patient could proceed to quantitative testing by venipuncture/automated method, whereas if AST or ALT was <3× ULN using the POC test, automated testing would not be indicated. Such use would save valuable clinical resources and time while still making triage testing available in remote areas. The work presented here indicates that our bin placement accuracies for the <3× ULN bin are nearly 100%. Our results for ALT (whole blood) indicate that no specimens with gold standard ALT values >120 U/liter were read by the paper-based test as <120 U/liter. For AST (whole blood), a small number of samples with gold standard AST values >120 U/liter were read by the paper-based test as <120 U/liter (Fig. 3D), indicating that further refinement of the assay is necessary. There were no specimens that had automated AST or ALT values >5× ULN that were read by

the paper assay as <3× ULN. This is important because TB treatment guidelines recommend that patients with levels >5× ULN stop their TB medications even if asymptomatic. We did not measure fingerstick specimens from patients with TB or HIV and thus cannot assess the performance of the device for measuring hepatotoxicity in those patients. Performance of the device at the bin cutoffs will need to be closely examined during real-time fingerstick testing of large numbers of such patients with elevated transaminases. A final limitation of our study is that we did not evaluate long-term (greater than 11 weeks) device stability, including at elevated temperatures.

Hepatotoxicity is a major adverse event associated with both antituberculous and antiretroviral therapy, and monitoring for drug-induced liver injury is accordingly a major priority in the care of these patients. Moreover, there are other important and common global conditions (such as epilepsy) for which treatment can be associated with substantial hepatotoxicity. We anticipate that our device will ultimately simplify and reduce the cost of detection and monitoring progression of hepatotoxicity, making extremely inexpensive, minimally invasive, and accurate transaminase testing available at POC for all who need it and thus providing distinct advantages over standard-of-care automated methods using venipuncture. Conceivably, our fingerstick test could also improve treatment adherence, given that aversion to venipuncture can be a barrier to completing TB treatment (9). Finally, successful development of this paper-based platform could facilitate the development of similar POC clinical assays for monitoring other clinically important analytes.

MATERIALS AND METHODS

Device fabrication
Device patterns were designed with Adobe Illustrator CS3. The pattern consisted of 12 rows of 9 devices for a total of 108 devices per sheet. Whatman No. 1 chromatography paper (8.5 × 11 inches) was fed into a laser printer (HP Color LaserJet 4520), and nine $0.85 × 14$–cm^2 yellow [Y = 100% on CMYK (cyan-magenta-yellow-black) scale] stripes were printed on the sheet. A wax pattern for the top layer (layer from which the device is read) was printed onto this sheet with a Xerox 8560DN printer such that the wax pattern was printed on the opposite side of the paper as the yellow stripe and that the yellow stripes only covered the back face of the ALT test zones and ALT negative controls in each column (that is, did not cover the back face of the AST test or AST control zones). The sheet was heated in a gravity convection oven at 150°C for 30 s. A wax pattern for the bottom layer (layer in contact with filters) was printed onto Whatman No. 1 chromatography paper with a Xerox 8560DN printer and heated in the oven at 150°C for 30 s. This layer did not have a yellow stripe on the reverse side of the paper.

A pressure-sensitive adhesive (Unitak 131, Henkel) was applied to the back of the top layer by screen printing such that the five active zones of the device did not receive adhesive but the remaining areas did. The layer was placed in a gravity convection oven set to 70°C for 15 min. This screen-printing and heating process was repeated on the back of the bottom layer. The sheets were then taped to a plastic frame to spot reagents. Details of the reagents used in each zone are provided in the Supplementary Methods. Zones were spotted with a micropipette according to fig. S1. Where multiple reagent spots were required, the first spot was allowed to dry completely (air dry at room temperature) before applying the second.

A hole puncher was used to punch alignment holes (preprinted on the corners of each sheet) in both device layers. The layers were aligned and laminated with a benchtop laminator (Apache AL13P) at a speed of 2 ft/min. Cold lamination (Fellowes self-adhesive laminate sheets) was then placed on the front face of the sheet of devices. An array consisting of 108 holes (each hole aligned with the center of a device), each with a diameter of 7 mm, was cut on a second sheet of laminate with a knife plotter (Craft ROBO Silhouette CC330L-20 SD) and placed on a bench adhesive side up. Precut discs (1 cm in diameter) of Pall Vivid GX plasma separation membrane were then centered on the holes in the laminate sheet in such a way that the rough side of the membrane was in contact with the adhesive. The cut laminate with adhered filters was then aligned and laminated to the back of the device sheet stack such that each filter covered all five zones of the device. Finally, the entire stack was laminated to ensure good contact between all layers. Individual devices were then cut by hand and stored in heat-sealed foil-lined bags containing one packet of silica desiccant (Sigma) with 10 devices per bag.

Visual read guide
The read guide (Fig. 1C) was generated by adding known amounts (as provided by the vendor) of AST and ALT (Lee Biosolutions) to fresh whole blood (drawn by venipuncture; baseline AST/ALT, 24/22 U/liter) to generate final concentrations of 40, 60, 80, 100, 120, 150, 180, 200, 250, 300, and 400 U/liter. Thirty microliters of the sample was added to each of three devices for all concentrations. After 15 min, the devices were scanned with a desktop scanner (Canon). Experiments were performed at room temperature (25°C). Images were analyzed with Adobe Illustrator CS3 to generate color swatches with the appropriate CMYK values. The read guide was printed and laminated between two Fellowes self-adhesive laminate sheets with a benchtop laminator (Apache AL13P).

Methods for linearity, LOD, repeatability, and stability experiments are described in the Supplementary Methods.

Experiments to evaluate potential interfering factors
Human serum samples with baseline AST/ALT levels measured by the supplier were obtained from Valley Biomedicals Inc. Purified ALT/AST (Lee Biosolutions) was then added to generate final levels of about 40 and 400 U/liter. Stock solutions of potential interfering reagents were prepared and added to the above ALT/AST serum samples at different final concentrations.

Collection and testing of clinical specimens
The protocol for access to discarded clinical specimens and associated clinical data was approved by the Investigational Review Board of Beth Israel Deaconess Medical Center (BIDMC). Routine clinical transaminase testing (AST/ALT) at BIDMC was performed on serum specimens by the BIDMC clinical chemistry laboratory with a Roche Modular Analytics System (P800 spectrophotometer module). Paired whole-blood (drawn in lavender–top EDTA tube) and serum (drawn in green–top heparin serum separator tube) specimens that were less than 5 hours old (time since venipuncture) were identified by searching electronically for reported serum AST and ALT results that spanned the clinical range and then confirming that a whole-blood specimen had been drawn from that patient at the same time. In total, 95 whole-blood and 128 serum specimens were selected for research testing; in some cases, either the whole-blood or the serum specimen from an original pair was no longer available. Aliquots (200 μl) of each specimen were removed, and these aliquots were de-identified. Aliquots (30 μl) of each de-identified spec-

imen were applied to individual devices by micropipette and allowed to sit at room temperature (range, 21 to 24°C). Fifteen minutes after application, results were read by eye in silence by three independent readers who were blinded to the results of automated transaminase testing of the serum specimens. Results were interpreted by comparing color changes in the ALT and AST test zones to the read guide, and results were recorded as values rounded to the nearest 10 U/liter. Control zone colors were checked to confirm proper device function. Whole-blood specimens were discarded after initial testing. Serum specimens were stored at 4°C for repeat testing.

Fingerstick specimens ($n = 10$) were obtained from healthy volunteers at Diagnostics For All, all of whom provided verbal consent after hearing a detailed explanation of the test procedure.

Statistical analysis

Pearson χ^2 test was used to compare proportions (bin placement accuracies), with $P < 0.05$ considered significant.

SUPPLEMENTARY MATERIALS

www.sciencetranslationalmedicine.org/cgi/content/full/4/152/152ra129/DC1
Methods
Fig. S1. Locations of spotted reagent solutions for ALT and AST assays.
Fig. S2. Evaluation of potential interfering factors.
Fig. S3. Paper assay results at various temperatures and read times.
Fig. S4. Bland-Altman plots of visual transaminase measurements from two different sample volumes.
Fig. S5. Room temperature stability of the paper-based transaminase test.
Table S1. ALT whole-blood raw data.
Table S2. AST whole-blood raw data.
Table S3. ALT serum raw data.
Table S4. AST serum raw data.
Table S5. Cost per device estimate for the paper-based transaminase test.

REFERENCES AND NOTES

1. J. J. Saukkonen, D. L. Cohn, R. M. Jasmer, S. Schenker, J. A. Jereb, C. M. Nolan, C. A. Peloquin, F. M. Gordin, D. Nunes, D. B. Strader, J. Bernardo, R. Venkataramanan, T. R. Sterling; ATS (American Thoracic Society) Hepatotoxicity of Antituberculosis Therapy Subcommittee, An official ATS statement: Hepatotoxicity of antituberculosis therapy. *Am. J. Respir. Crit. Care Med.* **174**, 935–952 (2006).
2. Panel on Antiretroviral Guidelines for Adults and Adolescents. *Guidelines for the Use of Antiretroviral Agents in HIV-1-Infected Adults and Adolescents* (Department of Health and Human Services, Washington, DC, 2012), pp. 1–161; http://www.aidsinfo.nih.gov/ContentFiles/AdultandAdolescentGL.pdf
3. A. Tostmann, M. J. Boeree, R. E. Aarnoutse, W. C. de Lange, A. J. van der Ven, R. Dekhuijzen, Antituberculosis drug-induced hepatotoxicity: Concise up-to-date review. *J. Gastroenterol. Hepatol.* **23**, 192–202 (2008).
4. J. M. McKoy, C. L. Bennett, M. H. Scheetz, V. Differding, K. L. Chandler, K. K. Scarsi, P. R. Yarnold, S. Sutton, F. Palella, S. Johnson, E. Obadina, D. W. Raisch, J. P. Parada, Hepatotoxicity associated with long- versus short-course HIV-prophylactic nevirapine use: A systematic review and meta-analysis from the Research on Adverse Drug events And Reports (RADAR) project. *Drug Saf.* **32**, 147–158 (2009).
5. E. Martínez, J. L. Blanco, J. A. Arnaiz, J. B. Pérez-Cuevas, A. Mocroft, A. Cruceta, M. A. Marcos, A. Milinkovic, M. A. García-Viejo, J. Mallolas, X. Carné, A. Phillips, J. M. Gatell, Hepatotoxicity in HIV-1-infected patients receiving nevirapine-containing antiretroviral therapy. *AIDS* **15**, 1261–1268 (2001).
6. L. K. Shipton, C. W. Wester, S. Stock, N. Ndwapi, T. Gaolathe, I. Thior, A. Avalos, H. J. Moffat, J. J. Mboya, E. Widenfelt, M. Essex, M. D. Hughes, R. L. Shapiro, Safety and efficacy of nevirapine- and efavirenz-based antiretroviral treatment in adults treated for TB-HIV co-infection in Botswana. *Int. J. Tuberc. Lung Dis.* **13**, 360–366 (2009).
7. C. J. Hoffmann, S. Charalambous, C. L. Thio, D. J. Martin, L. Pemba, K. L. Fielding, G. J. Churchyard, R. E. Chaisson, A. D. Grant, Hepatotoxicity in an African antiretroviral therapy cohort: The effect of tuberculosis and hepatitis B. *AIDS* **21**, 1301–1308 (2007).
8. Centers for Disease Control and Prevention (CDC), Severe isoniazid-associated liver injuries among persons being treated for latent tuberculosis infection—United States, 2004–2008. *MMWR Morb. Mortal. Wkly. Rep.* **59**, 224–229 (2010).
9. F. K. Shieh, G. Snyder, C. R. Horsburgh, J. Bernardo, C. Murphy, J. J. Saukkonen, Predicting non-completion of treatment for latent tuberculous infection: A prospective survey. *Am. J. Respir. Crit. Care Med.* **174**, 717–721 (2006).
10. A. W. Martinez, S. T. Phillips, G. M. Whitesides, E. Carrilho, Diagnostics for the developing world: Microfluidic paper-based analytical devices. *Anal. Chem.* **82**, 3–10 (2010).
11. A. W. Martinez, S. T. Phillips, E. Carrilho, S. W. Thomas III, H. Sindi, G. M. Whitesides, Simple telemedicine for developing regions: Camera phones and paper-based microfluidic devices for real-time, off-site diagnosis. *Anal. Chem.* **80**, 3699–3707 (2008).
12. A. W. Martinez, S. T. Phillips, M. J. Butte, G. M. Whitesides, Patterned paper as a platform for inexpensive, low-volume, portable bioassays. *Angew. Chem. Int. Ed. Engl.* **46**, 1318–1320 (2007).
13. A. W. Martinez, S. T. Phillips, G. M. Whitesides, Three-dimensional microfluidic devices fabricated in layered paper and tape. *Proc. Natl. Acad. Sci. U.S.A.* **105**, 19606–19611 (2008).
14. C. M. Cheng, A. W. Martinez, J. Gong, C. R. Mace, S. T. Phillips, E. Carrilho, K. A. Mirica, G. M. Whitesides, Paper-based ELISA. *Angew. Chem. Int. Ed. Engl.* **49**, 4771–4774 (2010).
15. Z. Nie, F. Deiss, X. Liu, O. Akbulut, G. M. Whitesides, Integration of paper-based microfluidic devices with commercial electrochemical readers. *Lab. Chip* **10**, 3163–3169 (2010).
16. J. L. Osborn, B. Lutz, E. Fu, P. Kauffman, D. Y. Stevens, P. Yager, Microfluidics without pumps: Reinventing the T-sensor and H-filter in paper networks. *Lab. Chip* **10**, 2659–2665 (2010).
17. E. Fu, B. Lutz, P. Kauffman, P. Yager, Controlled reagent transport in disposable 2D paper networks. *Lab. Chip* **10**, 918–920 (2010).
18. B. R. Lutz, P. Trinh, C. Ball, E. Fu, P. Yager, Two-dimensional paper networks: Programmable fluidic disconnects for multi-step processes in shaped paper. *Lab. Chip* **11**, 4274–4278 (2011).
19. E. Fu, P. Kauffman, B. Lutz, P. Yager, Chemical signal amplification in two-dimensional paper networks. *Sens. Actuators B Chem.* **149**, 325–328 (2010).
20. M. S. Khan, G. Thouas, W. Shen, G. Whyte, G. Garnier, Paper diagnostic for instantaneous blood typing. *Anal. Chem.* **82**, 4158–4164 (2010).
21. X. Li, J. Tian, G. Garnier, W. Shen, Fabrication of paper-based microfluidic sensors by printing. *Colloids Surf. B Biointerfaces* **76**, 564–570 (2010).
22. W. Dungchai, O. Chailapakul, C. S. Henry, Use of multiple colorimetric indicators for paper-based microfluidic devices. *Anal. Chim. Acta* **674**, 227–233 (2010).
23. E. M. Fenton, M. R. Mascarenas, G. P. López, S. S. Sibbett, Multiplex lateral-flow test strips fabricated by two-dimensional shaping. *ACS Appl. Mater. Interfaces* **1**, 124–129 (2009).
24. S. J. Vella, P. Beattie, R. Cademartiri, A. Laromaine, A. W. Martinez, S. T. Phillips, K. A. Mirica, G. M. Whitesides, Measuring markers of liver function using a micropatterned paper device designed for blood from a fingerstick. *Anal. Chem.* **84**, 2883–2891 (2012).
25. J. M. Bland, D. G. Altman, Measuring agreement in method comparison studies. *Stat. Methods Med. Res.* **8**, 135–160 (1999).
26. Cholestech Corporation, 510(k) substantial equivalence determination no. K032027.
27. Cholestech Corporation, *The Accuracy and Reproducibility of a Rapid, Fingerstick Method for Measuring Alanine Aminotransferase Is Comparable to Laboratory Reference Methods.* Technical Brief ML1255-01A (Cholestech Corporation, Hayward, CA, 2001).